Electronic Supplementary Material (ESI) for Journal of Materials Chemistry B.

Supporting Information

Antioxidative Myricetin Enriched Nanoparticles towards Acute Liver Injury

Tianyou Wang,[†a] Jianhua Zhang,[†a] Hengjie Zhang,[a] Wanjie Bai,[a] Jinhong Dong,[a] Zhen Yang,[a] Peng Yang,[a] Zhipeng Gu,[a] Yiwen Li,[a] Xianchun Chen[a] and Yuanting Xu*[a]*

[a]College of Polymer Science and Engineering, State Key Laboratory of Polymer Materials Engineering, Sichuan University, Chengdu 610065, China.

†These authors contributed equally to this work.

Materials

Myricetin (98 %) was purchased from DASF Bio-Technology Co. Ltd. (Nanjing, China). H_2O_2 (30%) and acetic acid (36 %) was purchased from Chengdu Jinshan Chemical Reagent Co. Ltd. (Chengdu, China). Arginine (99 %) and potassium persulfate (99.5%) were purchased from Shanghai Aladdin Bio-Chem Technology Co. Ltd (Shanghai, China). 2,2'-azino-bis (3-ethylbenzothiazoline-6-sulfonic acid) diammonium salt (ABTS, 98%) was purchased from TCI (Tokyo, Japan). Methanol, ethanol, N, N-Dimethylformamide (DMF) and dimethyl sulfoxide (DMSO) was purchased from Titan Technology Co. Ltd (Shanghai, China). All chemicals were used without further purification.

Quantum chemical computational

The energy levels of frontier molecular orbits including Highest Occupied Molecular Orbital (HOMO) and Lowest Unoccupied Molecular Orbital (LUMO) were calculated through DFT by Gaussian 09 package. The molecular orbits of possible moieties were imported at the B3LYP/6-31 G(d) level.[1]

Solution stability assay

The PMA-1 was as an example to test the solution stability in various mediums such as deionized water, phosphate buffered saline (PBS, pH=7.4) as well as culture medium (10 % fetal bovine serum in dulbecco's modified eagle medium). The NPs solutions in various mediums with the concentration of 0.5 mg/mL were cultured for different time up to 48 h. The sizes of PMA-1 NPs were evaluated by dynamic light scattering (DLS) and the optical images after 48 h were recorded, respectively. Furthermore, the NPs with the concentration of 0.5 mg/mL were prepared in various organic solvents such as methanol, ethanol, N, N-Dimethylformamide (DMF) and dimethyl sulfoxide (DMSO), and the behaviors of NPs were recorded as optical images.

ABTS scavenging assay

ABTS assay was then carried out to examine the antioxidative abilities in water, and the method was according to our previous work.[2] In short, 54.04 mg ABTS and 9.93 mg potassium peroxodisulfate was dissolved in deionized water, then the solution was mildly stirred in dark overnight at room temperature to obtain ABTS solution. 100 μL sample solutions (PMA-i, i=1-4, 1 mg/mL) and 100 μL ABTS solution were added into 2800 μL deionized water, respectively. The absorbance at 734 nm was recorded at different time points up to 30 min and the scavenging abilities was subsequently calculated. Then, the scavenging abilities with different sample concentrations were assayed after 30 min co-incubation.

H_2O_2 scavenging assay

H_2O_2 scavenging assay was then carried out to examine the antioxidative abilities in water, and the method was according to our previous work.[3] In short, 100 μL sample solutions (PMA-i, i=1-4, 1 mg/mL) were added into 2900 μL H_2O_2 solution (10 mM), respectively. The absorbance at 240 nm was recorded at different time points up to 30 min and the scavenging abilities was subsequently calculated. Then, the scavenging abilities with different sample concentrations were assayed after 30 min co-incubation.

Evaluation of HUVEC cell apoptosis by AO/EB staining

AO/EB dual staining was performed at a 1:1 ratio to evaluate the morphological changes of cells due to apoptosis. AO, which can pass through the plasma membrane, stains the DNA of live cells and fluoresces green. EB on the other hand is excluded from the cells having intact plasma membrane and stains the DNA of dead cells, showing orange fluorescence. After incubation, HUVEC cells were washed with PBS twice, stained with AO/EB (0.1 mg/mL) and observed under a fluorescence microscope at 200× magnification.

Characterization

Phenom Pro microscope was used for obtaining scanning Electron Microscope (SEM) images. Malvern Nano ZS ZEN3690 instrument was used for obtaining Hydrodynamic Diameter (DH) as well as Zeta Potential (ZP). FEI Tecnai F20 was used for obtaining electron energy-loss spectroscopy (EELS) mapping and the accelerating voltage was 200 kV. Flash EA 1112 was utilized to perform the organic element analyses of samples in dry states, and carrier, oxygen and reference gas flow rates were 140, 250 and 100 mL/min, respectively. The left, right furnace and oven temperatures are 900, 400 and 65℃, respectively. PerkinElmer Lambda 650 UV/Vis spectrophotometer was used for UV-vis spectra with slit of 2 nm. Applied Biosystems Biosystems API 2000 was used for electrospray ionization mass spectrometry (ESI-MS) spectrum with anion mode at a flow rate of 10 μL/min, spray voltage of 5 kV, auxiliary and sheath pressure of 45 psi. PHI Quantera SXM spectrometer using Al Ka radiation and spectra was used for X-ray photoelectron spectroscopy (XPS) at the pass energy of 160 eV for survey spectra and 20 eV high-resolution spectra of C 1s, O 1s, N 1s regions with the 300 ms dwell time. Bruker EPR EMX Plus was used for electron Paramagnetic Resonance (EPR) spectrum, and the spectrometer was performed at X-Band (9.85GHz) and 100 kHz field modulation at the power of 0.1 mW.

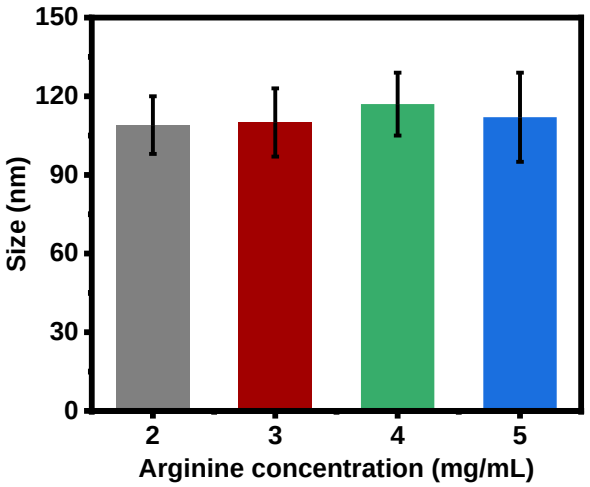

Fig. S1. Quantitative statistics of PMA-i (i=1-4) NPs sizes from SEM images, respectively.

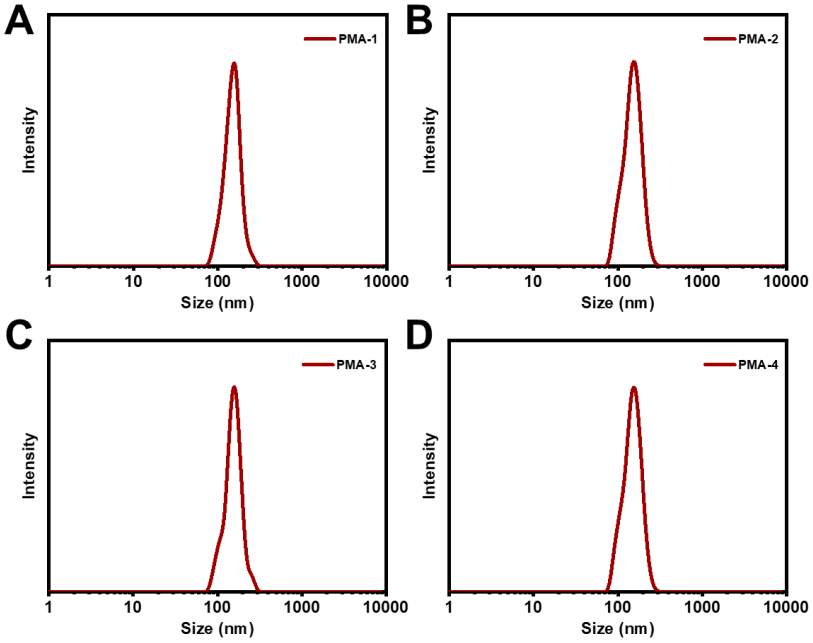

Fig. S2. Size distribution from DLS of PMA-i (i=1~4) NPs, respectively.

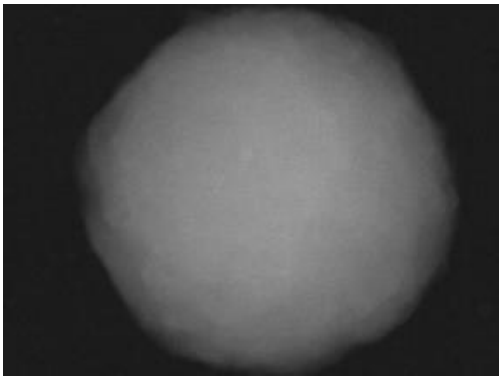

Fig. S3. Transmission electron microscope images of PMA-1 corresponding to the elements mapping shown in Fig. 1C.

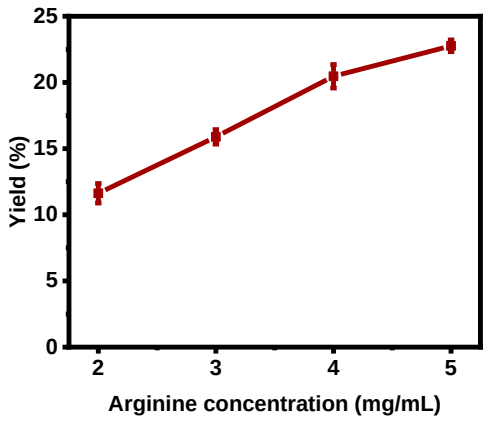

Fig. S4. The yields of NPs with different arginine concentrations.

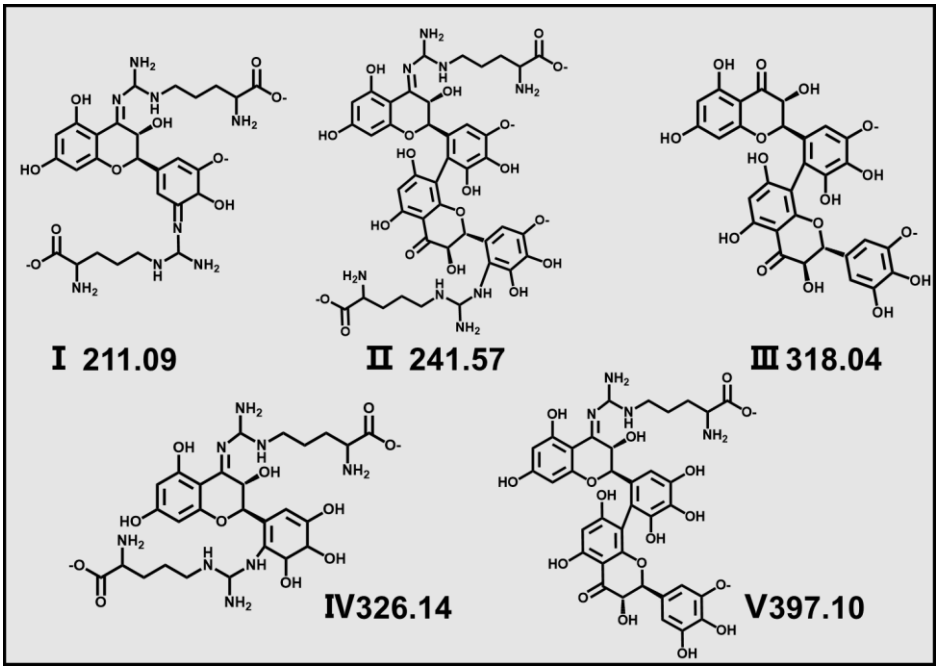

Fig. S5. The possible oligomer structures during the reaction process corresponding to the peaks shown in Fig. 1E.

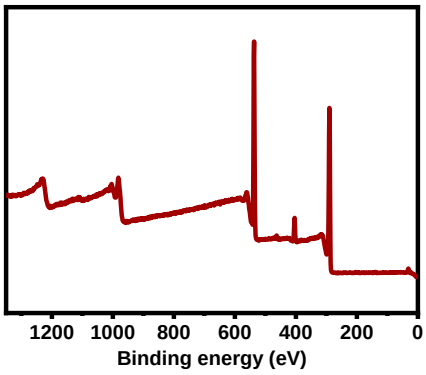

Fig. S6. The XPS curve of PMA-1.

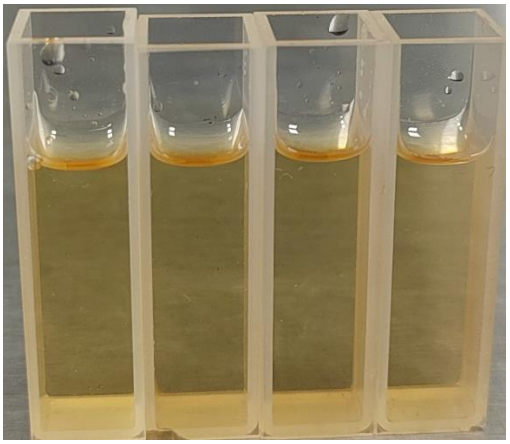

Fig. S7. The optical images of PMA-1 NPs in different solvents including methanol, ethanol, DMF and DMSO from left to right, respectively.

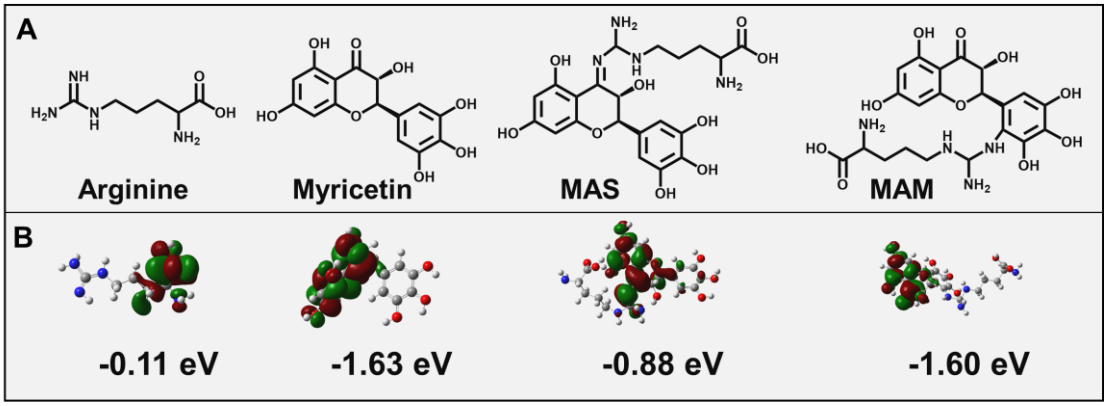

Fig. S8. The chemical structure and calculated lowest unoccupied molecular orbital (LUMO) energy levels of arginine, myricetin, MAS and MAM respectively.

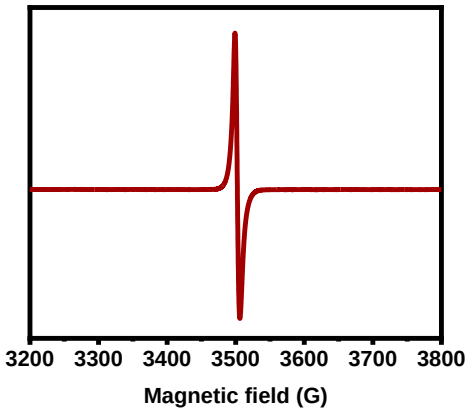

Fig. S9. The EPR spectrum of PMA-1 NPs.

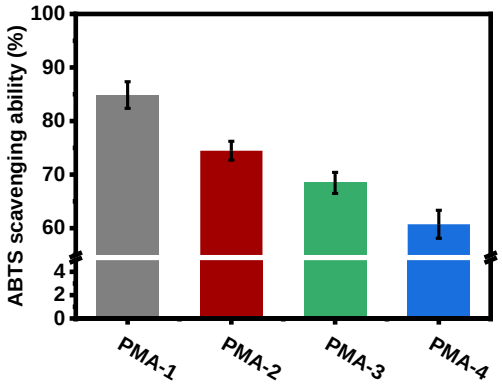

Fig. S10. The ABTS scavenging abilities of PMA-i (i=1-4) after 30 min co-incubation, respectively.

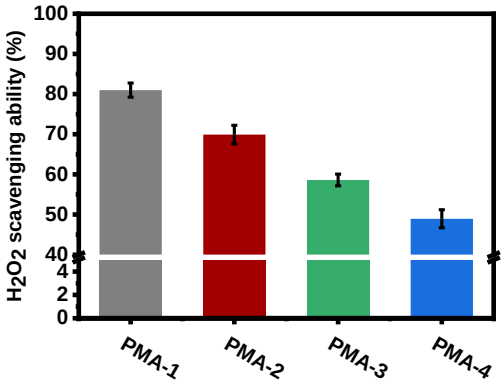

Fig. S11. The H_2O_2 scavenging abilities of PMA-i (i=1-4) after 30 min co-incubation, respectively.

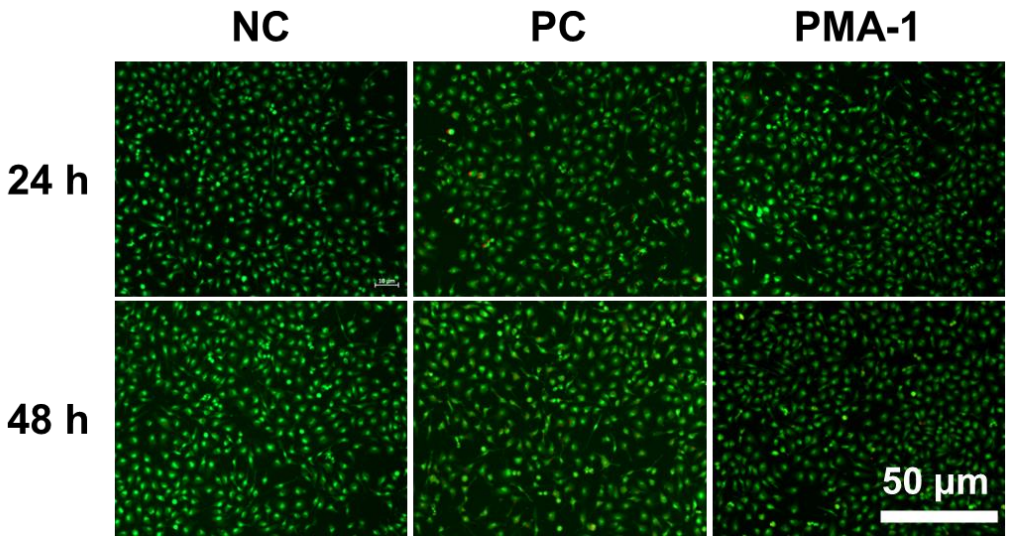

Fig. S12. The apoptosis analysis of NC, PC and PMA-1 groups, respectively.

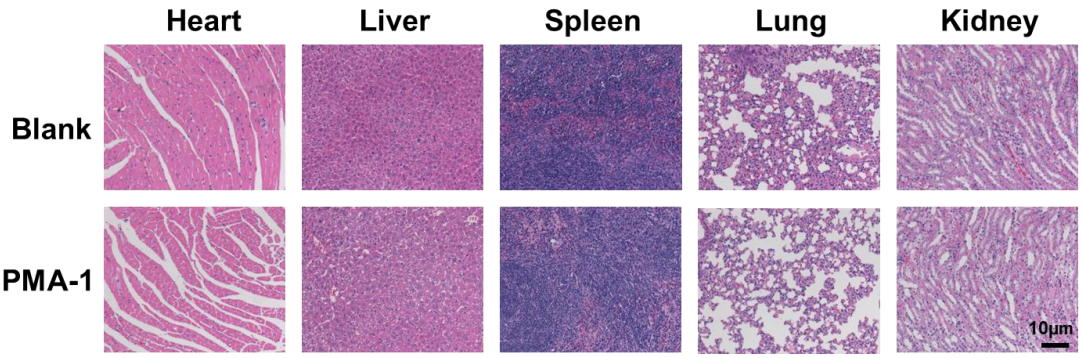

Fig. S13. The safety assessment of PMA-1 NPs *in vivo*.

Table S1. Specific parameters for the synthesis of PMA-i (i=1~4) NPs, respectively.

Sample	Arginine (mg)	Myricetin (mg)	Acetic acid (36 %, μL)
PMA-1	40	60	75
PMA-2	60	60	100
PMA-3	80	60	115
PMA-4	100	60	125

Table S2. Statistical parameters of prepared PMA-i (i=1~4) NPs.

Sample	$Size_{SEM}$ (nm)	$Size_{DLS}$ (nm)	PDI	Yield (%)
PMA-1	109±11	151	0.085	11.62
PMA-2	110±13	151	0.093	15.89
PMA-3	117±12	156	0.116	20.47
PMA-4	112±17	152	0.112	22.77

References

1. Frisch, M. J.; Trucks, G. W.; Schlegel, H. B.; Scuseria, G. E.; Robb, M. A.; Cheeseman, J. R.; Scalmani, G.; Barone, V.; Petersson, G. A.; Nakatsuji, H.; Li, X.; Caricato, M.; Marenich, A.; Bloino, J.; Janesko, B. G.; Gomperts, R.; Mennucci, B.; Hratchian, H. P.; Ortiz, J. V.; Izmaylov, A. F.; Sonnenberg, J. L.; Williams-Young, D.; Ding, F.; Lipparini, F.; Egidi, F.; Goings, J.; Peng, B.; Petrone, A.; Henderson, T.; Ranasinghe, D.; Zakrzewski, V. G.; Gao, J.; Rega, N.; Zheng, G.; Liang, W.; Hada, M.; Ehara, M.; Toyota, K.; Fukuda, R.; Hasegawa, J.; Ishida, M.; Nakajima, T.; Honda, Y.; Kitao, O.; Nakai, H.; Vreven, T.; Throssell, K.; Montgomery, J. A., Jr.; Peralta, J. E.; Ogliaro, F.; Bearpark, M.; Heyd, J. J.; Brothers, E.; Kudin, K. N.; Staroverov, V. N.; Keith, T.; Kobayashi, R.; Normand, J.; Raghavachari, K.; Rendell, A.; Burant, J. C.; Iyengar, S. S.; Tomasi, J.; Cossi, M.; Millam, J. M.; Klene, M.; Adamo, C.; Cammi, R.; Ochterski, J. W.; Martin, R. L.; Morokuma, K.; Farkas, O.; Foresman, J. B.; Fox, D. J. Gaussian 09, Revision A.02; Gaussian, Inc.: Wallingford, CT, 2016.

2. T. Wang, Q. Fan, J. Hong, Z. Chen, X. Zhou, J. Zhang, Y. Dai, H. Jiang, Z. Gu and Y. Cheng, *Small*, 2021, **17**, 2102485.

3. Z. Wei, L. Wang, C. Tang, S. Chen, Z. Wang, Y. Wang, J. Bao, Y. Xie, W. Zhao and B. Su, *Adv. Funct. Mater.*, 2020, **30**, 2002234.